QU XIYU
DONG XIAOFANG
LIU ZHEN
ZHANG SHOUPENG
WANG WEIQING
and
FANG ZHENGWEI

Experimental study on reservoir acidification and application effect of interstratified illite/smectite clay

This paper investigates and studies the advantages and disadvantages of existing acidification plans at home and abroad. In view of the high content of clay matrix in the glutenite reservoir, and in accordance with the mix proportion plan of "HF/HBF4+HCl+oxidants/additives", the author selects different types of chemical reagents and concentrations, and conducts hydrothermal experiments on smectite and illite by different acidification plans. In the light of mass loss and variation in ion concentration, it is determined through preliminary selection and optimal selection that the best acidification plan is "15%HCl +8%HBF_4 + 30%H_2O_2 + 9%NH_4F". The proposed acidification plan is applied to clay mineral samples purified from the cores and real core samples, and its effect is analyzed in the light of mass loss, permeability changes, variation in ion concentration, and with the aid of Scanning Electron Microscope (SEM). The experiment reveals that over 40% of the mixed clay minerals are corroded in the reaction, the core samples feature significant increase in the number of corrosion holes and fissures and exponential growth in permeability, and the corroded minerals are mainly interstratified illite/smectite (I/S) and illite. The findings demonstrate that the proposed acidification plan has a good effect on interstratified I/S clay.

Keywords: *Clay minerals, acidification experiment, application effect, oilfield development.*

Introduction

With the continuous improvement of exploration technology, China has entered the era of exploration of subtle oil and gas reservoirs (Li et al., 2004). As an important type of subtle oil and gas reservoir, glutenite reservoirs are distributed across the globe.

Typical examples include the Hemlock Formation of the McArthur River Oilfield in the U.S. (Elliott et al., 1971; Starzer et al., 1991; Schoffmann et al., 1991; O'Sullivan et al., 1991), Shahejie Formation of Jiyang Depression (Pan Yuanlin et al., 2003; Zan et al., 2011; Li et al., 2012; Xian Benzhong et al., 2014; Wang Shuping et al., 2014), etc. The glutenite reservoir is mainly developed in the steep slope zone of fault depressions. As the product of near-source rapid accumulation, it is characterized by low maturity of structure and composition, rapid rock-facies variation, strong reservoir heterogeneity and high matrix content (Zan et al., 2011). Due to the high mud content, the glutenite reservoir has a large amount of detrital clay minerals, which causes 70% of the total reservoir damage (Xie, 2007). As a result, the key to the development of glutenite oil reservoir lies in the selection of proper plug removal plan for the sensitive minerals (clay minerals) in the reservoir. At present, reservoir acidification is one of the most effective plug removal measures (Wang et al., 2002), and the existing acidification technologies at home and abroad have their own strong points and weaknesses (Table 1).

The glutenite reservoir is well developed in the steep slope zone of Jiyang Depression. Taking the steep slope zone in the north of Dongying Depression (Dongying North Zone) as an example, oil prospectors have made breakthroughs in glutenite fans in regions like Shanjiasi, Binnan, Lijin, Wangzhuang, Shengbei and Yanjia, and discovered such glutenite fan oil reservoirs as Yanjia oilfield, Yongan oilfield, Chenjiazhuang North Slope Oilfield, etc. The proved reserves account for more than 50% of the total oil and gas reserves in Dongying North Zone. The glutenite reservoirs of Dongying North Zone have high content of clay minerals, averaged at 10%. The content exceeds 10% in 33% of the samples gathered from this region. The clay minerals are mainly illite and interstratified I/S (Fig.1). In view of the high content of clay minerals and development difficulties of this region and in the light of the advantages and disadvantages

Messrs. Qu Xiyu, Dong Xiaofang and Liu Zhen, School of Geosciences & Technology, China University of Petroleum, Qingdao, Qu Xiyu, Laboratory for Marine Mineral Resources, Qingdao National Laboratory for Marine Science and Technology, Qingdao and Zhang Shoupeng, Wang Weiqing and Fang Zhengwei, Exploration and Development Research Institute of Sinopec Shengli Oilfield Company, Dongying, China. Email: quxiyu@upc.edu.cn

Table 1: Advantages and disadvantages of existing acidification technologies

Existing acidification technologies	Advantages	Disadvantages	Source
Mud acid acidification	Strong corrosion ability	Short penetration distance, high possibility of secondary precipitation	Willianms, 1983; Guo Wenying, 2006; Lv Baoqiang, 2014
Sequential injection of HCl-NH_4F	Low working cost, deep acidification	Complex technology, low corrosion capacity	Sevougian, 1992; Lv Baoqiang, 2014; Guo Wenying, 2006
Self-generating mud acid acidification	Slow reaction speed, deep acidification	High possibility of secondary pollution	Templeton, 1974; Gates, 1978; Guo Wenying, 2006
Buffer-regulated mud acid	Ability to resolve the no corrosion problem in high temperature wells and to avoid pollution from corrosion inhibitors	High possibility of formation plugging due to alkali metal precipitation of H_2SiF_6	Lybarger, 1978; Empleton, 1974; Guo Wenying, 2006
Organic mud acid technology	Low acid-rock reaction rate, retardance	High possibility of intensified metal corrosion due to secondary precipitation	Chris, 1997; Zhang Hong, 2010; Shu Yuhua, et al., 1999; Cheng Xingsheng et al., 1998
HBF_4 acidification technology	Slow reaction speed, stable particles	Relatively poor corrosion capacity	Chen Fu, 1996; Lv Baoqiang, 2014
Phosphoric acid-based retarded acid acidification technology	Ability to prevent corrosion, stabilize clay, and improve the chelation reaction of multivalent iron	Secondary precipitation of $Ca_3(PO_4)_2$	Zhang Jianli, 1996; Jiang Minglang, 1990; Guo Wenying, 2006
Aluminum salt retarded acidification	Low acid-rock reaction rate, deep acidification	Low corrosion capacity, high possibility of secondary precipitation	Cheng Lin, 2002; Jiang Minglang, 1990; Yang Yonghua, 2006
Solid nitric acid acidification technology	Strong corrosion ability, low corrosion rate	Low solubility of aluminosilicate minerals, difficulties and dangers in construction, high cost	Yang Yonghua, 2006; Cai Changyu, 2003; Wang Xinying, 2000; Liu Jie, 2003
"Multi-hydrogen acid" acidification technology	Slow reaction speed, deep penetration, inhibition of secondary precipitation	Slow reaction speed	Guo Wenying, 2006; Zhang Hong, 2010; Yu Bo, 2011; Zhang Ningxing, 2010

of existing acidification technologies at home and abroad, this paper selects an appropriate mix proportion plan for acidizing fluid, optimizes the acidification plan by acidizing illite and smectite under geothermal conditions, and determines the glutenite reservoir acidification plan applicable to interstratified I/S clay. After that, the authors conduct acidification experiment on the clay purified from the cores and core displacement experiment, and analyze the application effect of the optimized acidification plan based on the experiment results.

2. Experimental materials and methods

2.1 Experimental materials

2.1.1 Natural samples

The natural samples include 100% pure solid monomineralic samples of smectite and illite, reservoir core samples from Es4 in Dongying Depression (Table 2) and the mixed clay samples purified from the reservoir core samples.

Three core samples are selected. The contents of illite and interstratified I/S are negatively correlated, both of which are 93% at the maximum. The clay is purified in the following steps: select a target core sample, crush it to 200 mesh, and put the powder into a clean beaker; if the core is oily, wash

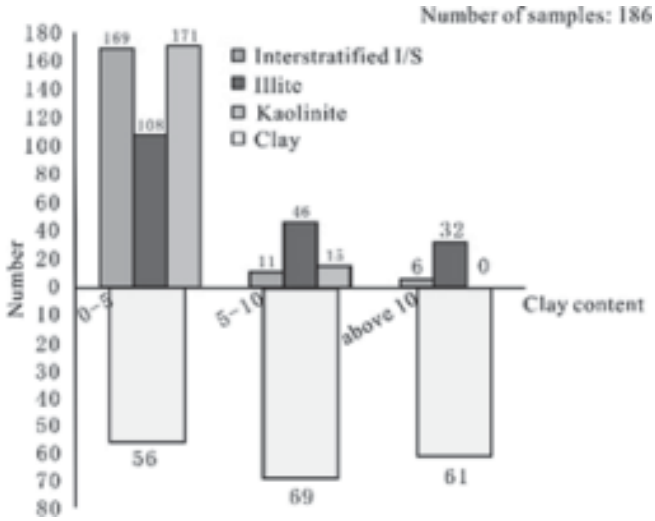

Fig.1 Histogram of clay mineral contents of glutenite reservoirs in Dongying North Zone of Jiyang Depression

the powder with alcohol to remove oil, rinse the oil-free powder with distilled water and filter the solution; if the core is oil-free, wash the powder with H_2O_2 to remove organic matters, rinse the inorganic powder with distilled water, and filter the solution till the solution is neutralized; add distilled

TABLE 2: X-RAY DIFFRACTION DATA OF CORE SAMPLES IN DONGYING NORTH ZONE

Well No.	Depth/m	Clay X-ray diffraction data %					Total rock X-ray diffraction data %								
		I/S	I	K	Ch	I/S ratio	Q	Kfs	Pl	Cal	Dol	Py	Anh	Sd	Clay
T198	3827.33		93	3	4		11	3	3	46	33		1		3
Y227	3280.50	40	58	1	1	30	30	22	32	5			2	3	6
Y96	1642.11	93	4	1	2	80	29	11	25	3	3	1	2		26

water into the filtered solution to obtain the clay suspension; let the clay suspension stand for 24 hours, and then evaporate the suspension to dryness to get the mixed clay; finally, identify the composition of the clay by X-ray diffraction analysis. In this research, the clay samples are purified from a total of 5 cores. Regarding the limitations on purification amount and experimental consumption, the confirmatory experiment of the acidification plan is solely based on the clay purified from the core of Tuo-98 well. The clay contains 57% of illite and 42% of interstratified I/S The book size will be in A4 (210 × 297 mm). Just as it is now, it uses custom margins: left margin 12.95 mm, right margin 12.95 mm, top margin 13.97 mm and bottom margin 20.06 mm. As the body text is divided into two columns in equal width (87.37 mm), the spacing between them is 8.89 mm. Please make sure that you do not exceed the indicated type area.

2.1.2 Chemical reagents

The chemical reagents include NH_4Cl, NH_4F and C_6H_5ONa solid powder; HCl (analytical grade) solution, HBF_4 solution, HF solution, H_2O_2 solution and CH_3COOH solution. The concentrations of the reagents are selected according to the following criteria:

2.1.2.1 Determination of acid concentrations

The HF concentration is determined as 3% due to its strong corrosion effect. If the concentration is greater than 3%, HF not only threatens the formation integrity, but also causes reservoir damages through the generation of K_2SiF_6, Na_2SiF_6, AlF_3, $KAlF_4$, Na_3AlF_6, etc. (Wang, 2002). The HCl concentration is determined as 15% because of the following reasons. HCl achieves a chemical balance with the above fluorine silicide and fluoride aluminide. If the HCl concentration is high or the ratio of HCl to HF is large, there is low probability of secondary damages (Wang Baofeng, 2001). However, excessively high ratio of HCl to HF would corrode the equipment and cause the precipitation of hydrated SiO_2. Summarizing experimental results (Wang, 2002), it is concluded that the most favorable HCl concentration for reservoir development is 15%. The HBF_4 concentration is determined as 8%. The reason goes as follows. Both HF and HCl are strong acid with excellent corrosion effect in the acidification process. The problem is the two acids are consumed too rapidly. HBF_4 offers a possible solution to the problem because of its ability to release HF through gradual hydrolysis, thus increasing the penetration distance of acidification by releasing HF, and its advantages of preventing clay and particle migration (Liu Xin, 2004), inhibiting clay expansion (Yue Jianghe, 2002; Wang Qiang, 2003), promoting the compressive strength of rock. Cao Yangshi et al. (1989) used HBF_4 to conduct a core corrosion experiment at the temperature of 80°C and the reaction time of 6h, and discovered that the core corrosion reaches the maximum rate when the HBF_4 concentration was 8%.

2.1.2.2 Selection of oxidants

The concentration of H_2O_2 is determined as 30% after comprehensive consideration of the oxidability of light components in crude oil, the viscosity of heavy oil and purchase cost. (See 2.2.1 for the specific procedures of the experiment.) The oxidability of H_2O_2 is strong enough to destroy the structure of layered silicate, and thereby promote the corrosion process (Wan Shiming et al., 2003). Besides, H_2O_2 can reduce the viscosity and improve the flowability of heavy oil through peroxide decomposition and heat release (Zheng Yancheng, 2009). The authors carried out a constant temperature water bath experiment to explore the viscosity reduction effect of H_2O_2 on heavy oil (Fig.2). It is found that the temperature of the water bath gradually rises (peak temperature 15°C) and the heavy oil viscosity falls as the H_2O_2 concentration increases. The maximum viscosity reduction rate (72.50%) appears when the concentration of H_2O_2 is 40%. However, the oxidation effect is still strong at this time, and the reduction rate is only slightly higher than that (69.36%) when H_2O_2 concentration is 30%.

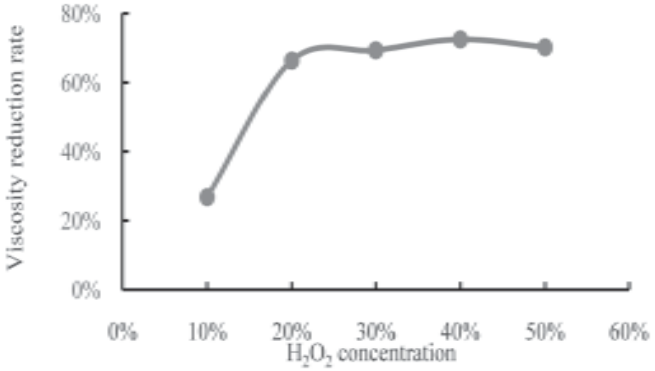

Fig.2 Relationship between H_2O_2 concentration and heavy oil viscosity reduction rate

2.1.2.3 Selection of additives

The additives selected in the study are NH_4Cl, NH_4F, CH_3COOH and C_6H_5ONa. NH_4Cl can prevent the precipitation of fluorosilicate, and reduce the formation plugging effect of fluorosilicate or fluoroaluminate by replacing other metal ions with ammonium ions. The NH_4Cl concentration is determined as 3% in this research (He, 2013). NH_4F can increase the concentration of free fluorine in the solution. Thanks to the ion exchange capacity of clay minerals, NH_4F can be combined with H+ on the clay surface to form HF, thus dissolving the clay from the surface (Wang, 2000). The NH_4F concentration is determined as 3%, 6% and 9% in this research. As an organic weak acid, CH_3COOH barely participates in reactions in the case of sufficient HCl. When a large amount of HCl is consumed, the organic acid is ionized to release H+, which produces HF through the reaction with fluorine complex. In this way, the HF reactivity is improved, the reaction is slowed down and the acidification is deepened (Yang, 2006). The CH_3COOH concentration is determined as 10% and 20% in this research. C_6H_5ONa can also curb precipitation because it is combined with cations to produce phenoxides. The C_6H_5ONa concentration is determined as 3%.

2.2 Experimental methods and processes

2.2.1 Constant temperature water bath experiment

A constant temperature water bath experiment is designed to verify the effect of H_2O_2 on reducing the viscosity of heavy oil. The specific steps are: put 100g crude oil into a beaker inserted with a thermometer; place the beaker in a constant temperature water bath, and adjust the temperature of the water bath to 50°C; add 1.5ml prepared solution of KI (ω: 20%) after the temperature of the crude oil in the beaker is stabilized, and stir the mixed solution evenly; add 4.8ml H_2O_2 (ω: 10%) solution, and stir the mixed solution evenly; record the highest temperature and measure the viscosity of the crude oil at the highest temperature. The experiment with H_2O_2 (ω: 10%) solution is wrapped up with the measured viscosity of the crude oil. Then, repeat the above steps, successively replace the 4.8ml H_2O_2 (ω: 10%) with 4.66ml H_2O_2 (ω: 20%), 4.5ml H_2O_2 (ω: 30%), 4.36ml H_2O_2 (ω: 40%) and 4.2ml H_2O_2 (ω: 50%), and record the viscosity of crude oil corresponding to each H_2O_2 concentration (Fig.2).

2.2.2 Clay mineral corrosion experiment

According to the mix proportion plan of "HF/HBF_4 + HCl + oxidants/additives", 29 acidification plans are prepared with the above chemical reagents of different concentrations. The plans are individually applied in the corrosion experiments of smectite and illite. The best acidification plan is determined through preliminary and optimal selection, and verified with the mixed clay purified from the core of Tuo-98 well. The experiment temperature is set as 150°C in light of the formation temperature of the Es4 in Dongying Depression (Yang, 1985); the experimental instruments include Teflon reactors with volume of 200ml and a KSY12-D-16 muffle furnace; the sample dosage is determined as: 5.82g smectite, 2g illite, 2g purified mixed clay, and 200ml acidification solution.

The preliminary selection has the following steps: place a certain amount of smectite into 87 reactors, divide the reactors equally into 3 groups (3×29), and add the 29 types of acidification solutions in a manner that ensures each reactor in the same group has a unique type of acidification solution. Seal up the reactors and move them group by group to the KSY12-D-16 muffle furnace. Heat up the first group of reactors at constant temperature for 1h, the second group for 2h, and the third group for 3h. After that, cool down the reactors and carry out solid-liquid separation of the mixture in each reactor. Finally, preliminarily select 3 types of acidification solutions based on the mass loss of the samples. The preliminary selection of acidification solutions for illite follows the same steps.

The optimal selection procedure is similar to that of the preliminary selection. Place a fixed amount of smectite into 15 reactors divide the reactors equally into 5 groups (5×3), and add the 3 types of preliminarily selected acidification solutions in a manner that ensures each reactor in the same group has a unique type of acidification solution. Let the acidification solutions react with smectite at constant temperature. The reaction lasts 1h in the first group of reactors, 2h in the second group, 3h in the third group, 6h in the fourth group and 12h in the fifth group. After the reactions, cool down and separate the mixture. Finally, determine the best acidification plan based on the mass loss of the samples and the ion concentration variation of the solutions in the reactions. The optimal selection of acidification solutions for illite follows the same steps.

The corrosion experiment of purified mixed clay is carried out in the following manner: Place the mixed clay and the best acidification solution into 5 reactors, and move the reactors into the KSY12-D-16 muffle furnace. Let the mixed clay react with the solution. The reaction lasts 1h in the first reactor, 2h in the second reactor, 3h in the third reactor, 6h in the fourth reactor and 12h in the fifth reactor. After that, cool down the reactors and carry out solid-liquid separation of the mixture in each reactor. Finally, discuss the corrosion effect of the acidification solutions based on the mass loss of the samples.

2.2.3 Core displacement experiment

3 core samples are selected in light of the X-ray diffraction data (Table 2), all of which has high illite and interstratified I/S contents. The authors carried out a core displacement experiment on the samples with the best acidification solution, compares the SEM features before and after the reaction, and discusses the actual effect of the solution based on permeability changes and variation in ion concentration. Fig.3 displays the instrument of the experiment: HKY-3 type core acidification system. The hastelloy (HC276) system works under the maximum pressure of 50MPa and maximum

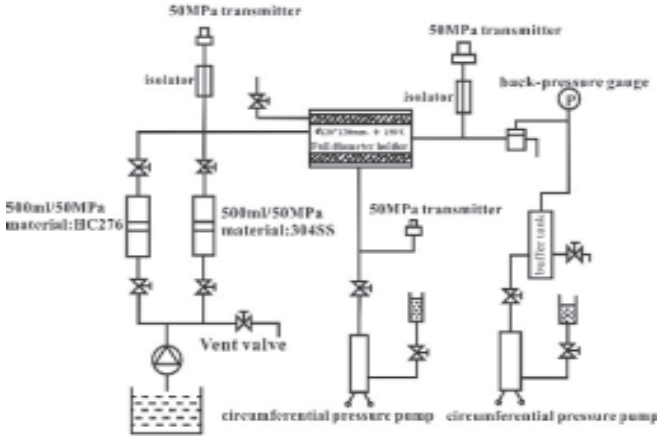

Fig.3 Components of the HKY-3 type core acidification system

temperature of 160°C. Prior to the reaction, the core samples are processed into cylinders with a diameter of 6.8cm with surfaces grinded smooth.

The process of the core displacement experiment goes as follows: put a cylindrical core sample into the plastic sleeve of the holder, seal up the holder, connect it to the components of the core acidification system, and apply the circumferential pressure; at room temperature, open the constant-flux pump to introduce the KCl (ω: 5%) to the core, and use the best acidification solution to displace the core; when the pressure is relatively stable, introduce KCl (ω: 5%) again to the core; the circumferential pressure should always be 2-3MPa greater than the displacement pressure so that all of the displacement solution flows through the core; when the flow is stabilized, record the difference between inlet and outlet pressures and the flow at the core; in view of core fluid parameters, calculate the core permeability before and after the acidification by the Darcy law, observe the sample with the scanning electron microscope before and after the reaction, and measure the post-reaction ion concentration of the solution.

3. Experimental study of acidification

In the study, a total of 204 experiments are carried out on monomineralic samples of smectite and illite, including 174 experiments for preliminary selection and 30 for optimal selection. In view of the limitation of space and the repetition of experimental data, the data of the preliminary selection experiments are omitted in this paper, and the results are given directly. The preliminarily selected acidification solutions for smectite are: 15% HCl + 8% HBF_4+ 30% H_2O_2 + 9% NH_4F, 15% HCl + 8% HBF_4+ 30% H_2O_2 and 15% HCl + 3% HF + 30% H_2O_2 + 3% NH_4F; preliminarily selected acidification solutions for illite: 15% HCl + 8% HBF_4 + 30% H_2O_2 + 9% NH_4F, 15% HCl + 3% HF + 10% CH_3COOH + 30% H_2O_2 + 3% NH_4F and 8% HBF_4 + 15% HCl + 30% H_2O_2.

3.1 Smectite acidification and corrosion experiment

The optimal selection is based on the thermostatic reactions between smectite and the 3 preliminarily selected acidification solutions: 15% HCl + 8% HBF_4 + 30% H_2O_2 + 9% NH_4F(M1), 15% HCl + 8% HBF_4 + 30% H_2O_2 (M2) and 15% HCl + 3% HF + 30% H_2O_2 + 3% NH_4F (M3).

3.1.1 Mass variation in the reaction

Fig.4 shows the corrosion-induced mass loss of smectite in the reaction. It can be seen that the HBF_4- containing acidification solutions (M1 and M2) exhibit much better corrosion effect than HF-containing acidification solution (M3). This means the combination of "HCl+HBF_4" is capable of ensuring the rate of corrosion and achieving the deep penetration. Within the HBF_4- containing acidification solutions, M1 has significantly better corrosion effect than M2, the maximum corrosion amount appears at 2h for both solutions, and the maximum corrosion-induced mass loss stands at 26.63%. The phenomenon is attributable to the addition of NH_4F. The additive is slowly hydrolyzed to form HF, which obviously intensifies the corrosion of smectite. The results demonstrate that the addition of NH_4F can achieve the effect of deep acidification.

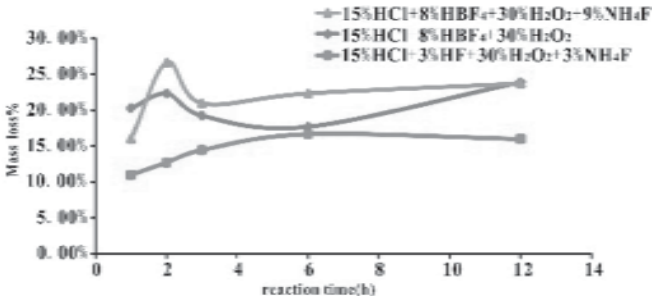

Fig.4 Mass loss % of smectite in the acidification and corrosion experiment

3.1.2 Ion concentration variation

In the reaction between smectite and the solutions, the concentration variation of Si^{2+} (Fig.5), Al^{3+} (Fig.6) and Mg^{2+} (Fig.7) is similar to that of the mass loss variation of smectite (Fig.4). The ion concentrations in M1 and M2 are higher than those in M3. Maximum ion concentrations appear in M1 at 2h: 812.5mg/l for Si^{2+}, 757.6mg/l for Al^{3+} and 224.6mg/l for Mg^{2+}. However, the peak ion concentrations appear at 1h instead of 2h in M2. This indicates that the corrosion rate is fast at the beginning in M2, but the rate falls and precipitation occurs as more and more acid is consumed; besides, the amount of precipitation is greater than the amount of corrosion. As the reaction time increases, the precipitates are dissolved after 6h. As a result, the ion concentrations increase rapidly and surpass those of M1 (Figs.6 and 7).

In the light of the corrosion effect, the acidification time (usually within 3h in oilfields) and other factors, M1 is determined as the best acidification solution and the best reaction time is set as 2h.

3.2 Illite acidification and corrosion experiment

The optimal selection is based on the thermostatic

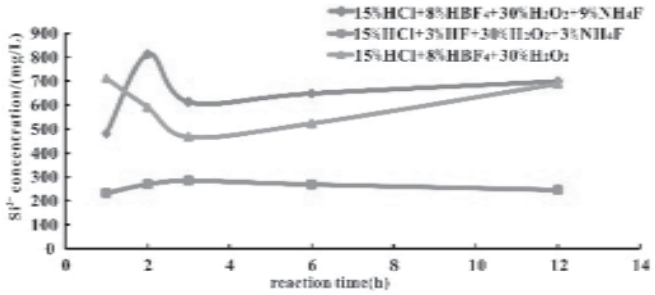

Fig.5 Si^{2+} concentration variation of smectite acidification and corrosion reaction liquid

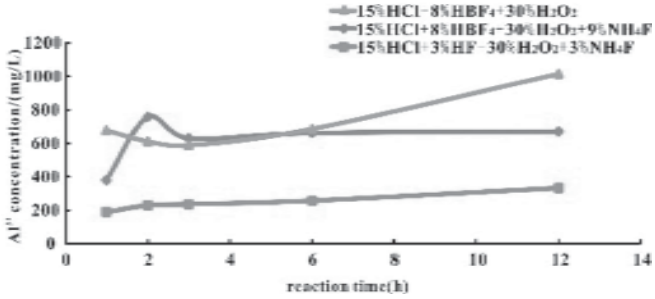

Fig.6 Al^{3+} concentration variation of smectite acidification and corrosion reaction liquid

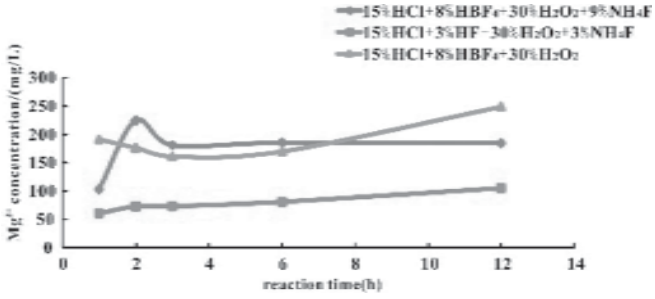

Fig.7 Mg^{2+} concentration variation of smectite acidification and corrosion reaction liquid

reactions between illite and the 3 preliminarily selected acidification solutions: 15% HCl + 8% HBF_4 + 30% H_2O_2 + 9% NH_4F (I1), 15% HCl + 8% HBF_4 + 10% CH_3COOH + 30% H_2O_2 + 3% NH_4F (I2) and 8% HBF_4 + 15% HCl + 30% H_2O_2 (I3).

3.2.1Illite mass loss

Fig.8 shows the corrosion-induced mass loss of illite in the reaction. Illite has less mass loss than smectite. The maximum mass loss of illite (23.45%) occurs at 6h in I3. In terms of mass loss, I2 has a poorer corrosion effect than the other two acidification solutions; it only does better than I1 at 6h. I1 boasts better corrosion effect than I3 in the first 2 hours, but falls behind from 3h. The gap keeps widening before 6h, but starts to shrink after the mass loss in I3 reaches the peak at 6h.

3.2.2 Ion concentration variation

In the reaction between illite and the solutions, the concentrations of Si^{2+} (Fig.9), Al^{3+} (Fig.10) and K^+ (Fig.11) vary in exactly the same trend similar to that of the mass loss variation of illite (Fig.8). The only difference lies in the fact that I3 has lower ion concentrations than the other two solutions at 3h. Maximum ion concentrations appear in M3 at 6h: 335.0mg/l for Si^{2+}, 404.0mg/l for Al^{3+} and166.2mg/l for K^+. According to the reaction time, the variation trend of Si^{2+}, Al^{3+} and K^+ can be divided into two stages. The first stage lasts from 0h to 4h, in which I1 has higher ion concentrations than I2 and I3, and the latter two have very close ion concentrations. The second stage starts from 4h, when the ion concentrations of I2 and I3 surpass those of I1. The concentrations continue to climb rapidly to the peak values at 6h. After that, the ion concentrations of I2 and I3 plunge right back to earth, and fall below those of I1 at 12h.

To sum up, I3 has the best corrosion effect in light of the corrosion-induced quality loss and ion concentrations, and

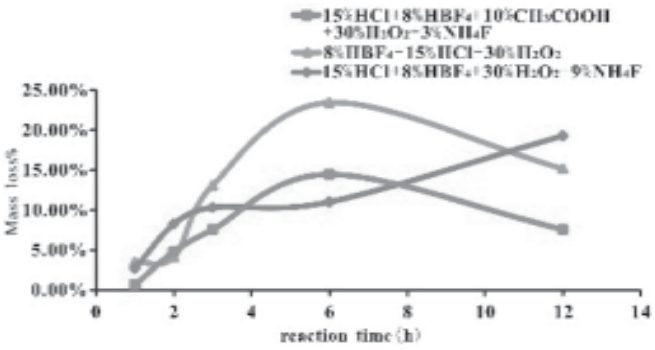

Fig.8 Mass loss % of illite in the acidification and corrosion experiment

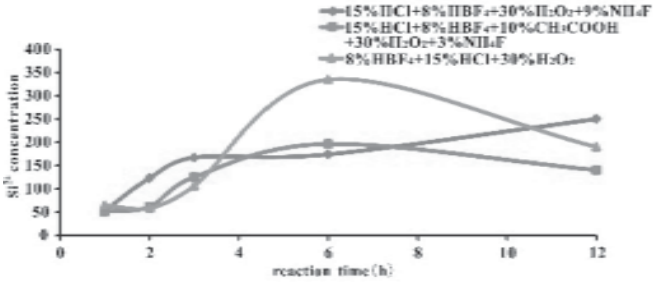

Fig.9 Si^{2+} concentration variation of illite acidification and corrosion reaction liquid

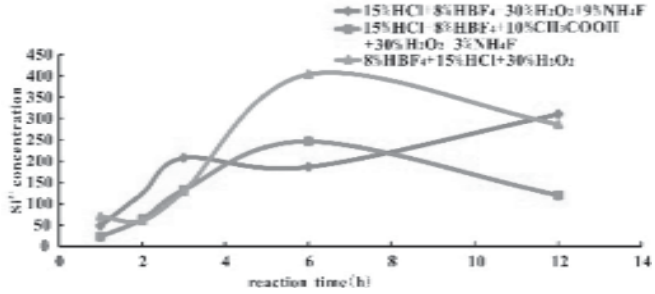

Fig.10 Al^{3+} concentration variation of illite acidification and corrosion reaction liquid

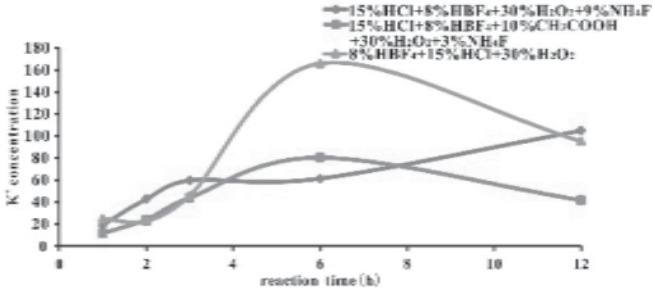

Fig.11 K^+ concentration variation of illite acidification and corrosion reaction liquid

the solution has optimal acidification effect at 6h. Considering the field acidification time and development cost, however, I1, with the optimal acidification time of 3h, is more suitable for practical application.

Through optimal selection, it is found that smectite and illite share the same best acidification plan: 15% HCl + 8% HBF_4 + 30% H_2O_2 + 9% NH_4F. Thus, the best acidification time is set as 2-3h.

4. Research on application effect

So far, 15% HCl + 8% HBF_4 + 30% H_2O_2 + 9% NH_4F has been identified as the best acidification plan through the preliminary and optimal selection of the acidification experiments on smectite and illite. In order to verify the application effect of the plan, the author conducts an acidification and corrosion experiment on the mixed clay purified from the cores, and a displacement experiment on natural cores.

4.1 Acidification and corrosion effect on the clay purified from the cores

The clay purified from the cores of Tuo-98 well is used to verify the acidification plan. The clay contains illite (57%) and interstratified I/S (42%). According to the mass loss of the purified clay in the reaction with the acidification solution (Fig.12), the acidification solution has a very prominent corrosion effect on the interstratified I/S clay. The mass loss is 43% at the minimum, and gradually increases with the reaction time. The 43.0-44.5% of mass loss in the best reaction time between 2h and 3h fully satisfies the acidification requirements for interstratified I/S clay reservoirs.

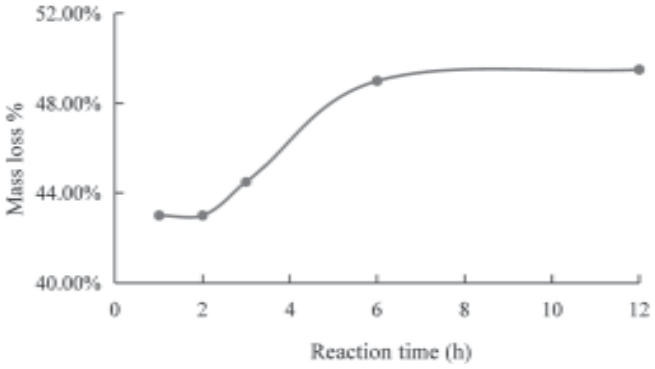

Fig.12 Mass loss % of purified clay in the acidification and corrosion experiment

4.2 Analysis of core acidification effect

In the study, the core samples of T198 (3,827.33m), Y227 (3,280.50m) and Y96 (1,642.11m) are subjected to displacement experiment using the HKY-3 type core acidification system and the best acidification solution. The corrosion characteristics of the cores are obtained by comparing the SEM features before and after the displacement, and the acidification effect is determined in view of the permeability variation in the displacement and post-reaction ion concentrations in the solution.

4.2.1 Core corrosion characteristics

Comparing the SEM features of core samples before and after the displacement, it is discovered that the number of corrosion holes (Fig.13A) and fissures (Fig.13B) on the samples has greatly increased. Apart from the corrosion of clay minerals, feldspar and carbonate minerals, there is also a certain amount of precipitates of new fluoride minerals.

The corrosion of clay minerals is dominated by the corrosion of interstratified I/S. The corrosion residues are flocculent (Fig.13C) or harbor-like (Fig.13D). The local corrosion is very strong, leaving only some residues of interstratified I/S (Fig.13E) and corrosion pores formed in the corrosion of illite (Fig.13F). The feldspar is heavily corroded, forming a large number of corrosion pores (Fig.13G) and corrosion residues (Fig.13E). The carbonate minerals are not severely corroded, except for the corrosion of calcite along the cleavage fissures. The corrosion of calcite is accompanied by the precipitation of CaF_2 (Fig.13H). CaF_2 and KF are two new minerals precipitated during the corrosion process. With heavy presence in local areas (Fig.13I), CaF_2 is flocculent and often associated with the corrosion of carbonate minerals (Fig.13H). The formation of CaF2 is probably related to the corrosion of calcareous minerals like calcite and plagioclase; the crystalline KF on the surface of the particles or filled in the pores (Fig.13J) must be formed by the participation of foreign ions because KCl solution is introduced during the displacement experiment.

To sum up, (1) in the core of Tuo-198 well, a number of corrosion holes can be observed but the number has not increased significantly in the displacement; the corrosion of illite and calcite is also observed, and CaF_2 precipitation occurs during the formation of secondary pores; (2) in the core of Yan-227 well, there is a significant increase of corrosion holes; the main corrosion targets are interstratified I/S and calcite; CaF_2 precipitates are observed during the corrosion of calcite; KF precipitation occurs in local areas; (3) in the core of Yi-96 well, the number of corrosion pores grows drastically and the main corrosion targets are interstratified I/S clay and feldspar.

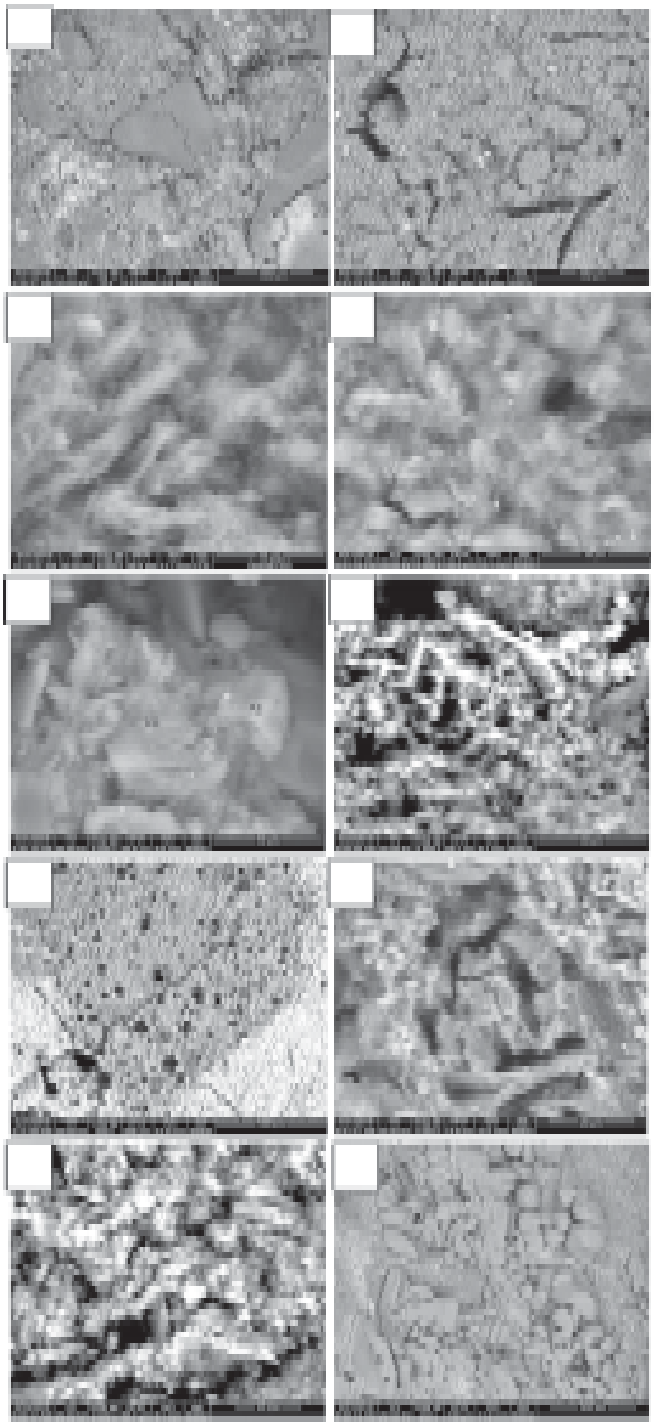

Fig.13 SEM images on mineral corrosion and precipitation after core displacement

A: The corrosion holes formed on the surface of particles (Y227, 3,280.50m); B: The corrosion fissures formed on the surface of particles (Y96, 1,642.11m); C: The flocculent corrosion residues of interstratified I/S (Y227, 3,280.50m); D: The harbor-like corrosion residues of schistose interstratified I/S (Y96, 1,642.11m); E: Corrosion residues of albite and interstratified I/S(Y96, 1,642.11m); F. The large number of corrosion holes formed in corrosion of feldspar (Y96, 1,642.11m); H. The corrosion holes of calcite and CaF_2 precipitates (Y227, 3,280.50m); I. The CaF_2 precipitates formed on the surface of particles (T198, 3,827.33m); J. KF precipitates formed on the surface of particles (Y227, 3,280.50m).

4.2.2 Core acidification effect

It can be inferred from the variation of ion concentrations in acidification (Fig.14) that the concentration of ions differ greatly from core to core after the acidification, especially for Ca^{2+} (max: 435.50μg/ml; min: 84.35μg/ml) and Al^{3+} (max: 62.57μg/ml; min: 7.75μg/ml). According to the X-ray diffraction data on core samples (Table 2), the core contains very few minerals that can produce Fe^{3+} (siderite, pyrite, etc.). Thus, the Fe^{3+} must be generated through the corrosion of metal components in the core acidification system. Moreover, with the introduction of KCl solution to the displacement process, it is deducted that K^+ comes from foreign sources rather than the corrosion of the cores. Therefore, Fe^{3+} and K^+ are excluded from the discussion below.

The concentration of Ca^{2+} and Mg^{2+} (Fig.14) is inversely proportional to the content of carbonate minerals (calcite and dolomite) (Table 2). Tuo-198 well boasts the highest concentration of carbonate minerals but the lowest concentration of Ca^{2+} and Mg^{2+}. As the content of feldspar and interstratified I/S increases, however, there is a gradual rise in the concentration of Ca^{2+} and Mg^{2+}. Yan-227, the well with the highest content of plagioclase, happens to feature higher concentration of Ca^{2+} and Mg^{2+} (83.57μg/ml) than the other two wells. Therefore, carbonate minerals are not the major source of Ca^{2+} and Mg^{2+}. Instead, Ca^{2+} is mainly produced in the corrosion of plagioclase, and Mg^{2+} in the corrosion of interstratified I/S clay. The concentration of Al^{3+} is proportional to the content of clay minerals, especially interstratified I/S. The highest Al^{3+} concentration is observed in Yi-96 well, the well with the highest content of interstratified I/S. This indicates that Al^{3+} mostly comes from the corrosion

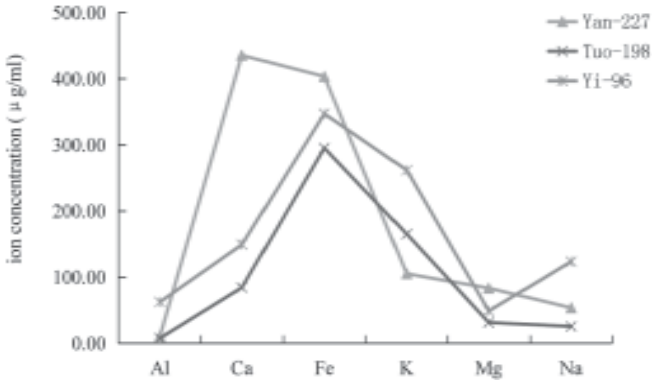

Fig.14 Variation of ion concentrations in the core displacement

of interstratified I/S clay. The variation pattern of Na^+ concentration is still vague. With plagioclase corrosion as the major source, the concentration of Na^+ is approximately proportional to the content of plagioclase. From the above analysis, it is clear that the best acidification solution has a desirable corrosion effect on clay minerals and a relatively weak corrosion effect on carbonate minerals.

Combining the results of SEM and ion concentration

analysis, it is concluded that the best acidification solution has a good corrosion effect on cores with high content of clay minerals, especially interstratified I/S. The finding is echoed by the comparison between the permeability before and after the reaction. The permeability of Yi-96 well and Yan-227 well, which contains higher levels of interstratified I/S, increases by 4 times and 3.04 times, respectively; In contrast, the permeability of Tuo-198 well, which contains higher level of carbonates, merely increases by 1.78 times. The contrast further proves that the acidification solution is an excellent acidifier for interstratified I/S clay, but is not sensitive to carbonate minerals.

5. Conclusions

(1) After reviewing the advantages and disadvantages of existing acidification plans in China and foreign countries, this paper decides to adopt the mix proportion plan of "HF/HBF_4 + HCl + oxidants/additives", and determines the concentrations and combinations of various chemical reagents.

(2) In light of the types of clay minerals of glutenite reservoirs in Dongying North Zone, the authors carried out 200+ hydrothermal experiments on smectite and illite according to 29 acidification plans, and selects "15% HCl + 8% HBF_4 + 30% H_2O_2 + 9% NH_4F" as the best acidification plan through the analysis of mass loss and the variation of ion concentrations.

(3) The effect of the best acidification plan is analyzed through the acidification and corrosion experiments on mixed clay purified from the cores and the displacement experiment. After the reaction, it is noted that over 40% of the mixed clay has been corroded; the number of corrosion holes and fissures of core samples has grown obviously; the corrosion is concentrated on minerals like interstratified I/S and illite but relatively weak on carbonates. Besides, the permeability of Yi-96 well and Yan-227 well, both of which have high content of interstratified I/S, increases by 4 times and 3.04 times, respectively; In contrast, the permeability of Tuo-198 well, which has high content of carbonates, merely increases by 1.78 times. The contrast confirms that the acidification solution is an excellent acidifier for interstratified I/S clay, but is not sensitive to carbonate minerals.

Acknowledgment

This research was supported by the National Natural Science Foundation of China (No. 41372133), Specialized Research Fund for the Doctoral Programme of Higher Education (No. 20090061120043), the Fundamental Research for the Central Universities (No. 12CX04004A).

References

1. Elliott, W. H. and Diver, C. J. (1971): "Early Reservoir Modeling of Trading Bay Unit Hemlock Formation," USA: Alaska.
2. Starzer, M. R., Unocal, O., Gas, D. and Borden, C. U. (1991): "Waterflood Monitoring Technique Results in Improved Reservoir Management for the Hemlock Reservoir, McArthur River Field, Cook Inlet, Alaska," USA: Anchorage, Alaska, pp.187-189.
3. Li, B. H., Li, Y. Q., Kong, D. B., Chen, Y. H., Fei, C. G. and He, Y. F. (2016): "Research on Influence Factors and Screening Method of Tight Sandstone Oil Reservoir CO_2 Huff and Puff Based on Multi-index," *Chemical Engineering Transactions*, vol.55, no.58, pp.343-348.
4. Schoffmann, A. B. and Marathon, O. C. (1991): "Optimizing Fracture Stimulations in the McArthur River Field, Hemlock Reservoir, Utilizing Historical Results and Improved Technology," *Anchorage*, Alaska, pp.635-639.
5. O'Sullivan, T. P. (1991): "Unocal Science and Technology Div," Kiloh, et al. Conglomerate Identification and Mapping Leads to Development Success in a Mature Alaskan Field, Anchorage, Alaska, pp.719-723.
6. Pan, Y. L., Zong, G. H., Guo, Y. X., Jiang, X. F. and Zhuo, Q. G. (2003): "Terrestrial Sequence Stratigraphy and Lithological Deposit Group of Sandstone in Jiyang Faulted Lacustrine Basin," *Acta Petrolei Sinica*, vol.24, no.3, pp.16-23.
7. Zan, L., Zhang, Z. H.,Wang, S. H., Feng, W. J., Zhang, L. S. and Xing, H. (2011): "Diagenesis of Sandy Conglomerate Reservoir in Northern Steep Slope of Bonan Subsag," *Natural Gas Geoscience*, vol.22, no.2, pp.299-306.
8. Zhao, X., Qiu, Z. S., Xu, J. G., Zhao, C. and Gao, J. (2017): "Flat-rheology oil-based drilling fluid for deepwater drilling," *International Journal Of Heat And Technology*, vol.35, no.1, pp.19-24.
9. Li, W. H., Zhang, Z. H., Zan, L. and Zhang, L. S. (2012): "Lower Limits of Physical Properties and Their Controlling Factors of Effective Coarse-grained Clastic Reservoirs in the Shahejie Formation on Northern Steep Slope of Bonan Subsag,the Bohai Bay Basin," *Oil & Gas Geology*, Vol.33, no.5, pp.766-777.
10. Xian, B. Z., Lu, Z. L., She, Y. Q., Wang, X., Wang, L. and Hang, H. D. (2014): "Sedimentary and Reservoir Characteristics of Glutenite in Yan 18 -Yong 921 Area, Steep Slope of Dongying Sag." *Lithologic Reservoirs*, vol.26, no.4, pp.28-35.
11. Wang, S. P., Xu, S. Y. , Dong, C. M., Wang, L. P. (2014): "Reservoir-space Characteristics and Genetic Mechanism of Deep Glutenite Reservoir of Es4x in the North Zone of the Dongying Depression," *Natural Gas Geoscience*, vol.25, no.8, pp.1135-1143.

12. Wang, B. F., Wang, X. G., Jiang, W. D., Xu, Z. H. and Zou, H. L. (2002): "The Research and Application of Acidification and Increasing Injection Technology for Low Pressure and Poor Injection," *Henan Petroleum*, vol.16, no.2, pp.12-17.
13. Williams, B. B. et al. and Luo, J. Q. translation (1983): "Oil well acidizing principle," Beijing, CHN: Petroleum Industry Press, 1983, pp.9-18.
14. Guo, W. Y. (2006): "The Study of Polyacetic Acidification Technology in Sandstone Reservoir," M.S.thesis, Dept.Electron.CN., Southwest Petroleum Univ., Chengdu, China.
15. Lv, B. Q., Li, X. P., Li, J. H., Pang, P. and Da, Y. P. (2014): "Application Situation of Reacidizing System in China," *Oilfield Chemistry*, vol.31, no.1, pp.136-140.
16. Sevougian, S. D., Lake, L. W. and Schechter, R. S. (1995): "A new geochemical simulator to design more effective sandstone acidizing treatments," *SPE Production & Facilities*, vol.10, no.01, pp.13-19.
17. Abrams, A., Lybarger, J. H., Richardson, E. A. and Neasham, J. W. (1978): "The Development And Application Of A High Ph Acid Stimulation System For A Deep Mississippi Gas Well," SPE Annual Fall Technical Conference and Exhibition, Houston, Texas, Tech.Rep.
18. Zhou, Q. H. and Yu, H. L. (2016): "Influence of Soil Surface Sodium Ion and Soil Ph on Dispersion of Cohesive Soil," *Chemical Engineering Transactions*, vol.55, pp.427-432.
19. Shuehart, C. E. (1997): "Chemical Study of Organic – HF Blends Leads to Improved Fluids," International Symposium on Oilfield Chemistry, Houston, Texas, Feb.18-21.
20. Zhang, H. (2010): "Feasibility Study on the Combination of Stratified Wells and Periodic Water Injection and Other," *Science & Technology for Development*, pp.178-187.
21. Shu, Y. H., Zhang, R. S. and Jiang, W. D. (1999): "Repeated Acidification and Increasing Injection Working Fluid in Ultra - deep Well of Lunnan Oilfield," *Driuing Fluid and Completion Fluld*, vol.16, no.1, pp. 12-14.
22. Cheng, X. S., Xu, Y., Chen, W. and Zhao, H. (1998): "Optimization and Application of Acid Fluid for Reacidizing Zhuangxi Arenaceous Carbonate," *Oil Drilling & Production Technology*, vol.20, no.6, pp.57-62+101-102.
23. Chen, F. and Yan, X. (1996): "The new progress Sandstone formation acidizing," *Drilling & Production Technology*, vol.19, no.3, pp.75-77+90.
24. Zhang, J. L., Wang, S. J. and Tang, F. M. (1996): "Slow acid acidification technology," *Tu Ha You Qi*, vol.1, no.1, pp.63-69.
25. Jiang, M. L. and Gao, C. L. (1990): "Retarded acidizing of sandstone reserviors by using aluminium salt as retarder(AIHF)," *Oilfield Chemistry*, vol.7, no.1, pp. 8-12.
26. Yang, Y. H., Hu, D. and Huang, Y. Z. (2006): "A New Stimulating Technique of Sandstone Reservoir:Acid Fracturing," *Fault-Block Oil & Gas Field*, vol.13, no.3, pp.78-80+94.
27. Cai, C. Y., Liao, D. Y. and Yan, Y. Z. (2003): "Nitric Acid Powder Acidizing Technology and Its Using in Field," *Driuing Fluid and Completion Fluld*, vol.20, no.4, pp.24-26+68.
28. Wang, X. Y., Song, Q. W. and Zheng, Y. (2000): "A Hydrogen Nitrate Powder Acidizing Technique," *Fault-block Oil and Gas field*, vol.7, no.3, pp. 54-56+71-72.
29. Li,. G. Z., Wang, Z. N., Liu, J., Lv, F. F., Zheng, L. Q. and Xiao, J. H. (2003): "Study of admix carboxylate oil flooding systems (?)-for high acid value oil," *China Surfactant Detergent & Cosmetics*, vol.33, no.6, pp. 350-355.
30. Yu, B., Tian, Y. H., Liu, X. W., Zhang, H. G., Li, X. M. and Yang, Y. G. (2011): "More acid hydrogen technology research and application," *Petrochemical Industry Application*, vol.30, no.7, pp.34-36+79.
31. Zhang, N. X. (2010): "Application of multi-hydrogen acidizing blocking removal technology in Huanxiling Oilfield," *Oil Drilling & Production Technology*, vol.32, no.6, pp.136-138.
32. Xie, F. M. (2007): "The Characterization of Glutinite Reservoir in Actic Region of Terrestrial Fault Basin-Example with Zhengnan-Lijin area," Ph.D. dissertation, Dept. Elect. CN, Chengdu University of Technology, Chengdu, China.
33. Templeton, C. C., Richardson, E. A., Karnes, G. T. and Lybarger, J. H. (1974): "Self-Generating Mud Acid (SGMA)," *Journal of Petroleum Technology*, vol.27, no.10, pp.1199.
34. Gates, H. R. and Lybarger, J. H. (1978): "Proper Reservoir Choice, Fluid Design Keys to SGMA Success," *Oil & Gas Journal*, vol.76, no.43, pp.137-138+141-142.
35. Emoleton, C. C., Street, E. H. and Richardson, E. A. (1974): "Dissolving Siliceous Materials with Self-Acidifying Liquid," *U.S.Patent* 3 828 854, Aug 13.
36. Magdalena, B., Stefan, D., Eva, S. and Barbora, P. (2016): "Study of Inorganic Pollution Sorption from Acidic Solutions by Natural Sorbents," *Chemical Engineering Transactions*, vol.53, pp.55-60.